JAERI-Research
97-052

ANALYSIS OF SPACE-TIME STRUCTURE OF INTERNAL TRANSPORT BARRIER IN JT-60U

August 1997

Sergei V. NEUDATCHIN*, Tomonori TAKIZUKA, Hiroshi SHIRAI
Takaaki FUJITA, Satoshi TAKEJI, Nobuaki ISEI and Yutaka KAMADA

日本原子力研究所
Japan Atomic Energy Research Institute

本レポートは，日本原子力研究所が不定期に公刊している研究報告書です。
入手の問合わせは，日本原子力研究所研究情報部研究情報課（〒319-11 茨城県那珂郡東海村）あて，お申し越しください。なお，このほかに財団法人原子力弘済会資料センター（〒319-11 茨城県那珂郡東海村日本原子力研究所内）で複写による実費頒布をおこなっております。

This report is issued irregularly.
Inquiries about availability of the reports should be addressed to Research Information Division, Department of Intellectual Resources, Japan Atomic Energy Research Institute, Tokai-mura, Naka-gun, Ibaraki-ken, 319-11, Japan.

編集兼発行　日本原子力研究所
印　　刷　いばらき印刷㈱

Analysis of Space-time Structure of Internal Transport Barrier in JT-60U

Sergei V. NEUDATCHIN*, Tomonori TAKIZUKA, Hiroshi SHIRAI
Takaaki FUJITA, Satoshi TAKEJI, Nobuaki ISEI and Yutaka KAMADA

Department of Fusion Plasma Research
Naka Fusion Research Establishment
Japan Atomic Energy Research Institute
Naka-machi, Naka-gun, Ibaraki-ken

(Received July 8, 1997)

Characteristics of the structure of Internal Transport Barrier (ITB) for reversed shear (RS) plasmas as well as for normal shear plasmas in JT-60U are studied. The fast-time-scale outward expansion of the ITB position is seen at the phase q_{min} passes across 3 in RS discharges. The steep features of the T_e and T_i profiles in RS plasmas are measured during the programmed-motion phase. The discontinuous change of the electron heat diffusivity χ_e within 3 cm distance near the ITB "shoulder" is found and the χ_e value in the ITB region is 1/10 of that inside the ITB "shoulder". It is observed that locations of the ITB for T_e and T_i are slightly different from each other. The BLM (Barrier Localized Mode) -induced L-H transition and the H-L back transition in a high β_p plasma with normal shear are studied. The BLM suddenly relaxes the T_e profile but does not deteriorate the improved transport property. The H-L back transition causes the simultaneous degradation of transport near the ITB region. The χ_e jump is estimated as about 1 m^2/s. After the back transition, the transport is discontinuously improved in time and the ITB properties are recovered. Global natures of these transient processes are noticeable. A new experimental technique called "multi-step programmed motion" is proposed to measure the steep structure of the ITB.

Keywords: Tokamak, JT-60U, Transport, Reversed Shear, Internal Transport Barrier, Heat Diffusivity, Barrier Localized Mode, L-H Transition, H-L Back Transition

---

* Nuclear Fusion Institute, Russian Research Center "Kurchatov Institute", Moscow, Russia

ＪＴ－６０Ｕにおける内部輸送障壁の空間・時間的構造の解析

日本原子力研究所那珂研究所炉心プラズマ研究部
Sergei V. NEUDATCHIN* ・滝塚　知典・白井　　浩
藤田　隆明・竹治　　智・伊世井宣明・鎌田　　裕

（1997年７月８日受理）

ＪＴ－６０Ｕ中の負磁気シアプラズマと通常磁気シアプラズマにおける内部輸送障壁の構造の特性を調べた。負磁気シア放電において，極小安全係数が３を切る時、内部輸送障壁の位置は速い時間スケールで外向きに拡がる。負磁気シアプラズマがプログラム化運動する時、電子温度とイオン温度の急峻な構造を測定した。内部輸送障壁の「肩」の近傍において、電子の熱拡散係数が３cm以内の距離で不連続的に変化する。その「肩」よりプラズマ中心側と比べて、内部輸送障壁の領域では電子熱拡散係数が１／10になっていることが分かった。電子温度とイオン温度に対する内部輸送障壁のそれぞれの位置は互いに少し異なっている。通常磁気シアの高β，プラズマにおけるＢＬＭ（障壁局在モード）誘起ＬＨ遷移とＨＬ逆遷移について調べた。ＢＬＭは内部輸送障壁領域の電子温度分布を急に緩和するが，改善輸送の性質を劣化させない。ＨＬ逆遷移は，内部輸送障壁近傍の輸送を同時的に劣化させる。この時の電子熱拡散係数の跳びはほぼ１m^2/sと評価された。逆遷移の後、輸送は時間に対して不連続的に改善され，内部輸送障壁の性質が回復する。これらの変動的輸送過程には全体的様相が見られる。内部輸送障壁の急峻構造を測定するために、「段階的プログラム化運動」と呼ぶ新しい実験手法を提案した。

那珂研究所：〒311－01　茨城県那珂郡那珂町向山801－１
＊ クルチャトフ研究所

Contents

1. Introduction 1
2. Evolution of ITB in RS Discharges 2
3. Programmed Motion in RS Discharges 3
3.1 Evolution of T_e and Reconstruction of "Real" Profile 4
3.2 Evolution of T_i 6
4. Study of BLM-induced Transitions 8
4.1 BLM-induced L-H transition and H-L Back Transition 8
4.2 Jump of Electron Heat Diffusivity 9
5. Discussion 11
6. Summary 11
Acknowledgments 12
References 13

目　　次

1. はじめに …… 1
2. 負磁気シア放電における内部輸送障壁の発展 …… 2
3. 負磁気シア放電におけるプログラム化運動 …… 3
3.1 電子温度の発展と実分布の再構築 …… 4
3.2 イオン温度の発展 …… 6
4. ＢＬＭ誘起遷移の研究 …… 8
4.1 ＢＬＭ誘起ＬＨ遷移及びＨＬ逆遷移 …… 8
4.2 電子熱拡散係数の跳び …… 9
5. 考　察 …… 11
6. まとめ …… 11
謝　辞 …… 12
参考文献 …… 13

1. Introduction

Recent success of JT-60U Reverse Shear (RS) experiments has been reported [1, 2]. A record value of the DT-equivalent fusion-power-amplification factor of $Q_{DT}^{eq} = 1.05$ was achieved [2]. The good confinement performance of these plasmas attributed the formation of the Internal Transport Barrier (ITB). The aim of the present paper is to highlight some features of the ITB formation in space and time for the reverse shear plasmas as well as for the normal shear plasmas.

The confinement properties of JT-60U plasmas are affected by various physical mechanisms under the various plasma conditions. The transition from L-mode to H-mode is observed when the loss power through the separatrix exceeds a threshold value [3]. The formation of the ITB occurs independently of the edge barrier formation for the peaked profile of deposition power in normal shear discharges [4]. The fast time scale and slow time scale global and local processes are involved into formation of the global confinement and local transport properties [5, 6, 7].

The transport analyses of normal shear discharges with ITB and especially of reverse shear discharges are complicated because of their small ($\Delta r/a_p \sim 0.1$) ITB width. In the RS discharges, the new type of ITB with clear pedestals of ion temperature T_i, electron temperature T_e, and electron density n_e was observed [1, 2]. The values of T_i, T_e and n_e are varied by 4-7 times in a distance Δr about 10% of minor radius a_p. Usually only one channel of the ECE grating polychromator [8] for the T_e measurement and one channel of the charge-exchange recombination spectroscopy (CXRS) [9] for the T_i measurement are located in the ITB region with steep temperature gradient. The toroidal rotation velocity V_t is also measured by the above CXRS We investigate the ITB features using mainly the fast time scale T_e measurement and medium time scale ($\geq$ 17 ms) T_i measurement described above.

In the present paper, we study the space-time structure of the ITB in reverse and normal shear discharges in JT-60U. We propose here an idea to study the ITB with the use of the programmed plasma motion. The time variation of the diagnostic positions "traveling through the ITB" due to the plasma motion enables us to measure the steep structure of the ITB. The programmed plasma motion has been applied to obtain the high performance plasmas during RS experiments in October of 1996 (including the shot E27969 with the highest Q_{DT}^{eq}) [10].

The fast-time-scale evolution or the expansion of the ITB without the programmed motion in RS discharges is shown in Section 2. Measurement of the steep features of T_e, T_i and V_t profiles during the programmed motion phase is described in Section 3. Discontinuous change of the conductivity in space around

the ITB is estimated, and the position of the "shoulder" of ITB is determined with the high space resolution. Problems for the reconstruction of the "real" T_e profile is discussed.

The physics of the ITB in normal shear plasmas has not fully been known yet. So-called Barrier Localized Modes (BLM) [11, 12] cause the fast-time-scale heat outflux to the plasma periphery. The study of a BLM-induced L-H transition for a high β_p pulse is described in Section 4. The relationship between the ITB transport property and the edge confinement is investigated. The electron conductivity jump in time is estimated for the fast-time-scale H-L back transition and for the fast-time-scale ITB recovery.

Discussion and summary are the contents of Sections 5 and 6, respectively. We propose for future JT-60U experiments a new technique called "multi-step programmed motion" to diagnose the ITB structure with less uncertainty in the reconstruction of the "real" profile.

2. Evolution of ITB in RS Discharges

Let us analyze the RS plasmas during JT-60U experiments in October of 1996. Waveforms of the RS discharge E27986 with increasing plasma current I_p up to 2.8 MA and the toroidal field B_t = 4.05 T are shown in Fig. 1. From the top to the bottom there are shown the plasma current I_p, the displacement of the plasma center in the major-radius direction DR, the stored energy measured by diamagnetic loop W_{dia}, the injected neutral beam power P_{NB}, T_e, T_i, and V_t. In this section, we analyze an interesting event seen 200-300 ms before t = 6.0 s in Fig. 1. The programmed inward motion started at the time t = 6.0 s, i.e., the displacement DR started to change with the inward velocity of about 10 cm/s.

The sudden rise of T_{e17} and the increase of T_{i12} correlated with the acceleration of V_{t12} are seen after t = 5.8 s. Here T_{e17} denotes the electron temperature measured on the 17th channel of the ECE grating polychromator, and T_{i12} (or V_{t12}) is the ion temperature (or the toroidal rotation velocity) measured on the 12th channel of the CXRS. Both of these channels are located near the "foot" of the ITB. On channels located in the core region inside the ITB "shoulder", a visible change in T_{e16} cannot be seen and no clear increase of T_{i11} is observed. Hereafter, we call the ITB outer boundary the "foot", and the ITB inner boundary the "shoulder", as illustrated in Fig. 2. Radial positions of the diagnostic channels are calculated by "SLICE" code with an MHD equilibrium given by "FBEQU" code [13]. The radial position of T_{e17} channel, r_{e17}, at t = 6.0 s is 0.703 m and r_{e16} = 0.606 m. The position of T_{i12} channel, r_{i12}, is 0.637 m and r_{i11} = 0.546 m. The volume averaged minor radius a_p is 1.04 m for this equilibrium. We suppose that this event was the expansion of the ITB, i.e., the radial position of the ITB abruptly moved

the ITB is estimated, and the position of the "shoulder" of ITB is determined with the high space resolution. Problems for the reconstruction of the "real" T_e profile is discussed.

The physics of the ITB in normal shear plasmas has not fully been known yet. So-called Barrier Localized Modes (BLM) [11, 12] cause the fast-time-scale heat outflux to the plasma periphery. The study of a BLM-induced L-H transition for a high β_p pulse is described in Section 4. The relationship between the ITB transport property and the edge confinement is investigated. The electron conductivity jump in time is estimated for the fast-time-scale H-L back transition and for the fast-time-scale ITB recovery.

Discussion and summary are the contents of Sections 5 and 6, respectively. We propose for future JT-60U experiments a new technique called "multi-step programmed motion" to diagnose the ITB structure with less uncertainty in the reconstruction of the "real" profile.

2. Evolution of ITB in RS Discharges

Let us analyze the RS plasmas during JT-60U experiments in October of 1996. Waveforms of the RS discharge E27986 with increasing plasma current I_p up to 2.8 MA and the toroidal field B_t = 4.05 T are shown in Fig. 1. From the top to the bottom there are shown the plasma current I_p, the displacement of the plasma center in the major-radius direction DR, the stored energy measured by diamagnetic loop W_{dia}, the injected neutral beam power P_{NB}, T_e, T_i, and V_t. In this section, we analyze an interesting event seen 200-300 ms before t = 6.0 s in Fig. 1. The programmed inward motion started at the time t = 6.0 s, i.e., the displacement DR started to change with the inward velocity of about 10 cm/s.

The sudden rise of T_{e17} and the increase of T_{i12} correlated with the acceleration of V_{t12} are seen after t = 5.8 s. Here T_{e17} denotes the electron temperature measured on the 17th channel of the ECE grating polychromator, and T_{i12} (or V_{t12}) is the ion temperature (or the toroidal rotation velocity) measured on the 12th channel of the CXRS. Both of these channels are located near the "foot" of the ITB. On channels located in the core region inside the ITB "shoulder", a visible change in T_{e16} cannot be seen and no clear increase of T_{i11} is observed. Hereafter, we call the ITB outer boundary the "foot", and the ITB inner boundary the "shoulder", as illustrated in Fig. 2. Radial positions of the diagnostic channels are calculated by "SLICE" code with an MHD equilibrium given by "FBEQU" code [13]. The radial position of T_{e17} channel, r_{e17}, at t = 6.0 s is 0.703 m and r_{e16} = 0.606 m. The position of T_{i12} channel, r_{i12}, is 0.637 m and r_{i11} = 0.546 m. The volume averaged minor radius a_p is 1.04 m for this equilibrium. We suppose that this event was the expansion of the ITB, i.e., the radial position of the ITB abruptly moved

outward. Such an ITB expansion with the fast time scale was observed in many similar RS pulses, but the most remarkable evolution of temperatures was seen for E27986.

Figure 3 shows waveforms of the RS pulse E27302 reported in Ref. [1]. In the period 5.35 s < t < 5.85 s, the H factor (confinement enhancement factor from ITER89P L-mode scaling) saturated with the increased MHD fluctuations of low toroidal mode numbers. During this phase, the value of q_{min} (minimum of the safety factor) passed across 3 [1]. The ion temperature on 10th channel, T_{i10}, drastically decayed at t = 5.4 s. The deceleration of V_{t10} accompanied with T_i decay. This event was explained in Ref. [1] as an inward movement or shrink of ITB. Taking into account of the T_e evolution, this event could be explained that a steep ITB gradient was relaxed into a little gentle gradient. Unfortunately the 15th channel of the ECE grating polychromator did not work in this shot, and therefore we cannot give a conclusive explanation so far. Here the radial positions of diagnostic channels at t = 5.7 s are r_{i10} = 0.54 m, r_{i11} = 0.63 m, r_{e15} = 0.58 m, r_{e16} = 0.68 m, and r_{e17} = 0.79 m in a plasma with a_p = 0.98 m.

Interestingly, after the decay of T_{i10} mentioned above, the temporary rises of T_{e16} and T_{i11} are seen for 5.6 s < t < 5.75 s in Fig. 3. Probably this event is the same process of the ITB expansion for the pulse E27986. A clear correlation with acceleration of the toroidal rotation is observed for T_{i11} located on the ITB outer boundary.

The mechanisms of above events connected with the ITB in RS discharges, i.e., the expansion of ITB position and the relaxation of ITB gradient, would be clarified in future.

Another kind of problem we found here is that the radial positions of the ion and electron channels near the ITB "foot" are systematically different with each other. For E27986 (Fig. 1), the "foot" of electron ITB, $r_{foot,e}$, assumed near the position of T_{e17} channel, r_{e17}, shifts by 6.5 cm outward from that of ion ITB, $r_{foot,i}$, near the position of T_{i12} channel, r_{i12}. For E27302 (Fig. 3), the shift, $r_{foot,e} - r_{foot,i} \approx r_{e16} - r_{i11}$, is about 5 cm. Whether this difference was caused by physical reasons or only by measurement uncertainties is a crucial question. This problem will also be discussed later.

3. Programmed Motion in RS Discharges

In this section, we discuss the period of the programmed plasma motion, i.e., t ≥ 6.0 s for RS discharges E27986, E27969 and E27975. The plasma center moves in the major-radius direction with the inward velocity, $|dDR/dt| \approx 10$ cm/s, as shown in Figs. 1, 4, and 5.

outward. Such an ITB expansion with the fast time scale was observed in many similar RS pulses, but the most remarkable evolution of temperatures was seen for E27986.

Figure 3 shows waveforms of the RS pulse E27302 reported in Ref. [1]. In the period 5.35 s < t < 5.85 s, the H factor (confinement enhancement factor from ITER89P L-mode scaling) saturated with the increased MHD fluctuations of low toroidal mode numbers. During this phase, the value of q_{min} (minimum of the safety factor) passed across 3 [1]. The ion temperature on 10th channel, T_{i10}, drastically decayed at t = 5.4 s. The deceleration of V_{t10} accompanied with T_i decay. This event was explained in Ref. [1] as an inward movement or shrink of ITB. Taking into account of the T_e evolution, this event could be explained that a steep ITB gradient was relaxed into a little gentle gradient. Unfortunately the 15th channel of the ECE grating polychromator did not work in this shot, and therefore we cannot give a conclusive explanation so far. Here the radial positions of diagnostic channels at t = 5.7 s are r_{i10} = 0.54 m, r_{i11} = 0.63 m, r_{e15} = 0.58 m, r_{e16} = 0.68 m, and r_{e17} = 0.79 m in a plasma with a_p = 0.98 m.

Interestingly, after the decay of T_{i10} mentioned above, the temporary rises of T_{e16} and T_{i11} are seen for 5.6 s < t < 5.75 s in Fig. 3. Probably this event is the same process of the ITB expansion for the pulse E27986. A clear correlation with acceleration of the toroidal rotation is observed for T_{i11} located on the ITB outer boundary.

The mechanisms of above events connected with the ITB in RS discharges, i.e., the expansion of ITB position and the relaxation of ITB gradient, would be clarified in future.

Another kind of problem we found here is that the radial positions of the ion and electron channels near the ITB "foot" are systematically different with each other. For E27986 (Fig. 1), the "foot" of electron ITB, $r_{foot,e}$, assumed near the position of T_{e17} channel, r_{e17}, shifts by 6.5 cm outward from that of ion ITB, $r_{foot,i}$, near the position of T_{i12} channel, r_{i12}. For E27302 (Fig. 3), the shift, $r_{foot,e} - r_{foot,i} \approx r_{e16} - r_{i11}$, is about 5 cm. Whether this difference was caused by physical reasons or only by measurement uncertainties is a crucial question. This problem will also be discussed later.

3. Programmed Motion in RS Discharges

In this section, we discuss the period of the programmed plasma motion, i.e., t ≥ 6.0 s for RS discharges E27986, E27969 and E27975. The plasma center moves in the major-radius direction with the inward velocity, $|dDR/dt| \approx 10$ cm/s, as shown in Figs. 1, 4, and 5.

During the phase of inward plasma motion, radial positions of diagnostic channels move outward. The radial velocity of the position of k-th diagnostic channel, $v_k \equiv dr_k(t)/dt$, is not simply determined as $v_k = -dDR/dt$, but determined from equilibrium calculations for many time points. The time evolution of the "measured" temperature on the k-th channel, $T_k(r_k(t), t)$, is the result of the time-space variation of the "real" temperature profile, $T(r, t)$;

$$\frac{d}{dt} T_k(r_k(t), t) = \frac{\partial}{\partial t} T(r, t) + v_k \frac{\partial}{\partial r} T(r, t) \quad . \tag{1}$$

For the steady-state profile, $\partial T/\partial t = 0$, the "measured" temperature decays in time with the outward motion of diagnostic-position, $v_k > 0$, because the temperature usually decreases in space, $\partial T/\partial r < 0$.

3.1 Evolution of T_e and reconstruction of "real" profile

The non-monotonic decay is found on both T_{e16}, T_{e17} and T_{i12} channels during 6.0 s < t < 6.3 s in Fig. 1 for E27986. The first decay from t = 6.0 s may correspond mainly to the radial gradient of temperature, i.e., the second term in the right hand side (RHS) of Eq. (1). The rise of T_e and T_i after t = 6.1 s can be considered to be the temporal increase, i.e., the first term in the RHS of Eq. (1), caused by the ITB expansion as the same as the event described in Section 2. When the diagnostic positions of T_{e16}, T_{e17} and T_{i12} moved out of the ITB for t > 6.3 s, the change of "measured" temperature became small.

Figure 4 shows waveforms of the RS pulse E27969 (the highest Q_{DT}^{eq} shot). The different behaviors of "measured" temperatures, T_{e13} and T_{e14}, are clearly seen. The decrease of T_{e14} was obvious for 6.6 s < t < 7.0 s, while T_{e13} increased gradually. Such waveforms were observed reproducibly for the similar RS discharge E27975 as shown in Fig. 5.

Let us study in detail the space and time variation of T_e for E27969. The evolution of radial positions and T_e values for 13th and 14th channels are given in Fig. 6. The MHD equilibria of the moving plasma analyzed here are obtained from calculations by the FBEQU code. Points on a curve from inner to outer are plotted at every 0.1 s from t = 6.0 s to t = 7.3 s. For the estimation of the temperature gradient $\partial T_e/\partial r$, one of the simplest ways is the use of a differential approximation;

$$\left(\frac{\partial T_e}{\partial r}\right)_{r = (r_{e13} + r_{e14})/2} \approx \frac{T_{e14} - T_{e13}}{r_{e14} - r_{e13}} \quad . \tag{2}$$

The maximum gradient estimated from this approximation with data points at t = 7.1 s is $|\nabla T_e|_{max} \approx |(3600 - 7800) / (60.5 - 49.5)| = 380$ eV/cm.

The temperature gradient can be estimated also by using a "measured" temperature, whose diagnostic position is moving. The evolution of T_{e14} in space exhibits the ITB structure as clearly seen in Fig. 6. Sometimes such an estimation gives more accurate values compared with a differential approximation. The relation between the "real" T_e profile and values of $T_{ek}(r_{ek}(t), t)$ "measured" by k-th channel with the radial velocity v_{ek} is derived from Eq. (1) as follows;

$$\frac{\partial}{\partial r} T_e(r, t) = \frac{1}{v_{ek}} \left(\frac{d}{dt} T_{ek}(r_{ek}(t), t) - \frac{\partial}{\partial t} T_e(r, t) \right)$$

$$= \frac{d}{dr} T_{ek}(r_{ek}(t), t) - \frac{1}{v_{ek}} \left(\frac{\partial}{\partial t} T_e(r, t) \right) , \qquad (3)$$

$$T_e(r, t_0) = T_{ek}(r_{ek}(t), t) - \int_{t_0}^{t} dt' \left(\frac{\partial}{\partial t'} T_e(r, t') \right) , \qquad (4)$$

$$\text{with} \quad r_{ek}(t) - r_{ek}(t_0) = \int_{t_0}^{t} v_{ek}(t') \, dt' .$$

The left hand sides of Eqs. (3) and (4) are the "real" ∇T_e and T_e, respectively. The first terms in the RHS are "measured" values from curves as drawn in Fig. 6. The "real" ∇T_e and T_e values are equal to the "measured" values only for the stationary T_e profile. The second terms in the RHS are the correction terms for unsteady case. If the speed of the channel position is enough high as $|v_{ek}| >> L/\tau$, the "measured" T_e profile agrees well with the "real" one, where L is the size of the measurement region and $\tau \approx |\partial \ln T_e/\partial t|^{-1}$ is the characteristic time of T_e evolution. If the speed is not so high, we need to evaluate the time derivative $\partial T_e/\partial t$ by examining the evolution of T_e on neighboring channels. Strictly speaking, it is not always possible to reconstruct a T_e profile for the general case.

Now we discuss the reconstruction of the "real" T_e profile from the "measured" profile for Figs. 4 and 6. At first, the ∇T_e values are estimated by using the differential approximation, Eq. (2). In the core region inside the ITB, the ∇T_e value is obtained from T_{e14} and T_{e13} for 6.0 s $\leq t \leq$ 6.5 s as ∇T_e = -10 eV/cm. Near the inner "shoulder", the ∇T_e value is obtained from T_{e14} and T_{e13} at t = 6.6 s as ∇T_e = -63 eV/cm, and the ∇T_e value in the ITB region is estimated as ∇T_e = -380 eV/cm from T_{e14} and T_{e13} at t = 7.0 s.

Secondly, the ∇T_e values are estimated by using the "measured" value of dT_{e14}/dr. It becomes about -450 ev/cm for 6.7 s < t < 6.9 s, which is the

"uncorrected" ∇T_e value in the ITB region. This absolute value is larger by ~20% than that estimated by the differential approximation at t = 7.0 s.

We evaluate the correction described in Eq. (3). The time derivative in the core region with $\nabla T_e \approx$ -10 eV/cm is approximately given by using T_{e13} behavior, $\partial T_e/\partial t \approx dT_{e13}/dt - v_{e13} \nabla T_e$. The value of dT_{e13}/dt for 6.2 s < t < 6.8 s is about 2700 eV/s (see Fig. 4), and the velocity v_{e13} is about 15 cm/s which is faster than |dDR/dt| $\approx$ 10 cm/s (see Fig. 6). Accordingly, we obtain $\partial T_e/\partial t \approx 2700 + 15 \times 10 = 2850$ eV/s. If we assume that the time derivative in the ITB region is nearly the same as that in the core region, then we obtain the correction value as $\Delta(\nabla T_e) \equiv -(\partial T_e/\partial t) / v_{e14} \approx -2850 / 18 \approx -160$ eV/cm where $v_{e14} \approx 18$ cm/s is calculated from Fig. 6. Therefore the limits of the correction can be 0 eV > $\Delta(\nabla T_e)$ > -160 eV. The maximum gradient in the ITB region is 450 eV/cm < $|\nabla T_e|_{ITB}$ < 610 eV/cm. This value is 7~10 times larger than that inside the ITB "shoulder", $|\nabla T_e| < 63$ eV/cm.

Based on the above analysis, we obtain the radial profile of the "real" $|\nabla T_e|$ near the ITB "shoulder" as shown in Fig. 7, where a possible band of the profile is given. The characteristic length for the change in the profile, $\lambda \equiv \nabla T_e / \nabla(\nabla T_e)$, is found to be $\lambda = (2.2 \pm 0.5)$ cm. It is obvious from all the above results that the discontinuous change of ∇T_e near the ITB "shoulder" is occurred in the distance shorter than the spatial resolution of 3.3 cm for the 14th channel of the polychromator.

It can be considered that the spatial changes in the electron density n_e and the absorbed power density Q_{abs} are smaller than that of ∇T_e. Therefore, the value of electron heat diffusivity χ_e is evaluated to be almost inversely proportional to the ∇T_e value. We expect the discontinuous change of χ_e near the ITB "shoulder", and very small χ_e value in the ITB region which is 1/10 of that inside the ITB "shoulder. Careful analysis will be done in future by taking account of profiles of n_e and Q_{abs}.

Finally we analyze the T_e evolution in the time interval of 7.0 s $\leq$ t $\leq$ 7.3 s. It is shown on Fig. 6 that the position of 14th channel stops during 7.0 s $\leq$ t < 7.2 s, and that the inward motion is seen for t > 7.2 s. The "measured" value of the ∇T_e estimated for 7.2 s < t < 7.3 s is -750 ev/cm, whose absolute value is 1.7 times higher in comparison with $|\nabla T_e|$ estimated for 6.7 s < t <7.0 s. The possible causes of such a $|\nabla T_e|$ enhancement are that P_{NBI} was increased from 13 to 17 MW at t = 6.9 s, and that the ITB is moved outward. We will discuss about this phenomenon also in the next subsection.

3.2 Evolution of T_i

The different behavior of the T_i signals from 8th and 9th CXRS channels, T_{i8} and T_{i9}, is clearly seen in Fig. 4 (E27969). The decrease of T_{i9} in time for 6.5 s < t <

7.0 s corresponds to the traveling of 9th-channel position through the ITB, while the constant value of T_{i8} suggests that 8th-channel position does not reach the ITB "shoulder". These behaviors are similar with the behaviors of T_{e14} and T_{e13}, respectively. The variation in time of the radial positions and T_i values for channels 8, 9 and 10 are plotted in Fig. 8, where the T_{e14} data from Fig. 6 are also presented for comparison. The channel 10 was already on the ITB at the beginning of column motion at t = 6.0 s. The channel 9 arrived at the ITB "shoulder" at t ≈ 6.5 s, while the channel 8 remains outside of the ITB. The ITB widths for T_i and T_e seems almost the same and ≤ 10 cm.

The increase of T_{i9} for t > 7.0 s suggests the outward motion of the ITB region, whose location can be seen by drawing a line from a point of $T_{i9}(t)$ to a point of $T_{i10}(t)$ in Fig. 8. At this phase, the outward motion of the ITB for T_e is also observed as was mentioned in the former subsection.

The radial profiles of T_i obtained from many channels at three moments, t = 6.0 s, 6.77 s and 7.3 s, for E 27969 are shown in Fig. 9. Outward shift of the ITB region from t = 6.77 s to t = 7.3 s is clearly seen. The profiles of V_t are also shown in the figure. The positions of the minimum velocity (or maximum of absolute value) seem to be located at the ITB "shoulder". The clear correlation between the vanishing point of strong shear flow and the ITB "foot" for T_i is found. On the other hand, the shear-flow region extends to the inner region from the ITB "shoulder" for T_i. One of the candidates of this reason is that the shear flow is generated not only by ∇T_i but also by ∇T_e. The ITB for T_e seems to shift inward from the ITB for T_i as will be mentioned below.

Interestingly, a small difference is observed in the ITB locations between for T_e and T_i. The T_{i9} reaches the ITB "shoulder" at t ≈ 6.5 s on r ≈ 0.45 m, while the T_{e14} reaches the ITB "shoulder" at t ≈ 6.7 s on r ≈ 0.54 m. Such a difference is also seen for the nearly identical pulse E27975 (case of Fig. 5). As was discussed in section 2, the location of the ITB "foot" for T_e is found to shift outward by about 5 cm from that for T_i. It seems that both the ITB "foot" and "shoulder" for T_e are located at outer positions compared with those for T_i, respectively.

The diagnostic positions were determined by the FBEQU calculation, where the value of safety factor q at the magnetic axis is chosen unity. To examine whether the FBEQU calculation causes the above difference, we recalculate the positions of channels by using a "FBEQUNG" code in which the q profile is chosen nearly realistic. Though the recalculated positions, r_{i9} and r_{e14}, for both T_{i9} and T_{e14} are shifted outward about 7 cm from the FBEQU-calculation results, the change in the distance $r_{e14} - r_{i9}$ is small, i.e., $r_{e14} - r_{i9} \approx 7$ cm for FBEQU calculation and $r_{e14} - r_{i9} \approx 5.5$ cm for FBEQUNG calculation. With the use of more realistic

profiles of pressure and q, accurate equilibrium calculations will be necessary to clarify whether the distance can be reduced or not.

The other possible reasons for this difference are 1) physical difference of ITB positions, 2) physical difference of ITB gradients due to banana size, and different spatial resolutions between T_{i9} (~ 6 cm) and T_{e14} (~3 cm). Because of 2) and 3) reasons, the 9th channel of CXRS can "feel" the ITB structure smooth and wide in comparison with T_{e14}. This important problem should be clarified in future.

4. Study of BLM-induced Transitions

The influence of the BLM on the ITB characteristics is analyzed. The BLM has been considered to be one of MHD instabilities driven by the steep pressure gradient at the ITB [11, 12]. It was found that the BLM relaxes the temperature profile inside the ITB and causes the increase of peripheral temperature. The L-H transition is sometimes induced by this BLM event [11]. In this section, we describe a BLM-induced L-H transition in the high β_p discharge E23612 of normal shear plasma. Some properties of this shot was reported in Ref. [14] from the viewpoint of the necessary heating power for the ITB creation. It should be noted in high β_p discharges with normal shear configuration that the clear ITB structure is formed for T_i and n_e, but the T_e has no clear ITB structure. We use here the word of "ITB region" as the region where the ITB for T_i is formed.

4.1 BLM-induced L-H transition and H-L back transition

The waveforms of the shot E23612 are shown in Fig. 10. The plasma current I_p is 1.4 MA, the toroidal field B_t is 4.4 T, and the volume averaged minor radius a_p is 0.90 m. The stored energy W_{dia}, injected neutral beam power P_{NB}, line integrated electron density n_eL, D_α signals from and away from the divertor region, and electron temperature T_e for channels 7 and 6 are shown in the figure. Arrows indicate the times of transitions described bellow; A) BLM at t = 5.895 s, B) H-L back transition at t = 5.921 s, C) first recovery at t = 5.968 s, and D) second recovery at t = 6.015 s.

Fast-time-scale polychrometer data of T_e are presented in Fig. 11. Radial positions of channels are r/a_p = 0.14 for ch. 11, r/a_p = 0.33 for ch. 13, r/a_p = 0.44 for ch. 7, r/a_p = 0.56 for ch. 6, r/a_p = 0.68 for ch. 5, r/a_p = 0.79 for ch. 16, and r/a_p = 0.98 for ch. 17. Channels 6 and 7 ($0.4 < r/a_p < 0.6$) are located near the ITB region. Time evolution of T_i with rather slow time resolution is shown in Fig. 12, where radial positions of channels are r/a_p = 0.31 for T_{i4}, r/a_p = 0.43 for T_{i6}, r/a_p = 0.53 for T_{i7}, r/a_p = 0.63 for T_{i8}, r/a_p = 0.74 for T_{i9}, r/a_p = 0.85 for T_{i10}, and r/a_p = 0.98 for T_{i11}.

Sudden decay of T_e is induced by the BLM at the time A, t = 5.895 s as clearly seen on T_{e6} and T_{e7} located inside the ITB, $0.4 < r/a_p < 0.6$. The decay is

profiles of pressure and q, accurate equilibrium calculations will be necessary to clarify whether the distance can be reduced or not.

The other possible reasons for this difference are 1) physical difference of ITB positions, 2) physical difference of ITB gradients due to banana size, and different spatial resolutions between T_{i9} (~ 6 cm) and T_{e14} (~3 cm). Because of 2) and 3) reasons, the 9th channel of CXRS can "feel" the ITB structure smooth and wide in comparison with T_{e14}. This important problem should be clarified in future.

4. Study of BLM-induced Transitions

The influence of the BLM on the ITB characteristics is analyzed. The BLM has been considered to be one of MHD instabilities driven by the steep pressure gradient at the ITB [11, 12]. It was found that the BLM relaxes the temperature profile inside the ITB and causes the increase of peripheral temperature. The L-H transition is sometimes induced by this BLM event [11]. In this section, we describe a BLM-induced L-H transition in the high β_p discharge E23612 of normal shear plasma. Some properties of this shot was reported in Ref. [14] from the viewpoint of the necessary heating power for the ITB creation. It should be noted in high β_p discharges with normal shear configuration that the clear ITB structure is formed for T_i and n_e, but the T_e has no clear ITB structure. We use here the word of "ITB region" as the region where the ITB for T_i is formed.

4.1 BLM-induced L-H transition and H-L back transition

The waveforms of the shot E23612 are shown in Fig. 10. The plasma current I_p is 1.4 MA, the toroidal field B_t is 4.4 T, and the volume averaged minor radius a_p is 0.90 m. The stored energy W_{dia}, injected neutral beam power P_{NB}, line integrated electron density n_eL, D_α signals from and away from the divertor region, and electron temperature T_e for channels 7 and 6 are shown in the figure. Arrows indicate the times of transitions described bellow; A) BLM at t = 5.895 s, B) H-L back transition at t = 5.921 s, C) first recovery at t = 5.968 s, and D) second recovery at t = 6.015 s.

Fast-time-scale polychrometer data of T_e are presented in Fig. 11. Radial positions of channels are r/a_p = 0.14 for ch. 11, r/a_p = 0.33 for ch. 13, r/a_p = 0.44 for ch. 7, r/a_p = 0.56 for ch. 6, r/a_p = 0.68 for ch. 5, r/a_p = 0.79 for ch. 16, and r/a_p = 0.98 for ch. 17. Channels 6 and 7 ($0.4 < r/a_p < 0.6$) are located near the ITB region. Time evolution of T_i with rather slow time resolution is shown in Fig. 12, where radial positions of channels are r/a_p = 0.31 for T_{i4}, r/a_p = 0.43 for T_{i6}, r/a_p = 0.53 for T_{i7}, r/a_p = 0.63 for T_{i8}, r/a_p = 0.74 for T_{i9}, r/a_p = 0.85 for T_{i10}, and r/a_p = 0.98 for T_{i11}.

Sudden decay of T_e is induced by the BLM at the time A, t = 5.895 s as clearly seen on T_{e6} and T_{e7} located inside the ITB, $0.4 < r/a_p < 0.6$. The decay is

rather slow and small amount for T_{e13} and T_{e11}, which are located at a distance from the ITB, $r/a_p < 0.4$. On the other hand, the fast jump of T_{e5}, T_{e16}, and T_{e17} is observed outside the ITB, $r/a_p > 0.6$. The T_i is varied in similar manner, i.e., decay of T_i for $r/a_p < 0.6$ and increase for $r/a_p > 0.7$.

The neutral influx is abruptly enhanced by the BLM-induced plasma outflux. The fast jumps of n_eL and D_α signal away from the divertor region ($D_{\alpha 5}$ in Fig. 10) are observed. The D_α signal from the divertor region $D_{\alpha 10}$, however, drops correlating with the BLM. Gradual increase of n_eL and edge T_i after the D_α drop, $t >$ 5.895 s, is also observed. These phenomena suggest an L-H transition being induced by the BLM.

It is interesting that the T_e profile near the ITB region is soon reconstructed within about 20 ms, i.e., values of T_{e6} and T_{e7} return to almost the same values as those before the BLM crash. This fast recovery suggests that the BLM does not deteriorate the improved transport property near the ITB. On the other hand in the evolution of T_{i6} and T_{i7} near the ITB region, we do not see the aspect of the recovery. It has not been clear so far whether no recovery of T_i really happened or the small recovery was hidden by the slow resolution of CXRS measurement. This problem should be clarified in future.

The rebuilding of the T_e profile is clearly interrupted at the time B, $t = 5.921$ s. The T_e starts to decay simultaneously with D_α jump. We classify this event as an H-L back transition. Near the ITB, the decay of T_{e6} and T_{e7} is obvious. The decrease of T_{e16} and T_{e17} near the edge is also seen but is not clear. A time delay of the T_e response is observed for the inner channels as was described in the previous study of L-H-L transitions in JT-60U [5]. These T_e responses show the global nature of the transport property. The edge T_i decay is also appeared on T_{i10}, T_{i11}. An interruption of the density rise is noticed also. The decay of W_{dia} becomes faster after $t = 5.921$ s, i.e., the energy confinement time is suddenly decreased by this H-L back transition.

4.2 Jump of electron heat diffusivity

The global response of T_e during the H-L back transition is caused by the global change in the electron heat diffusivity χ_e [5, 6, 7]. The jump of χ_e in time, $\delta\chi_e \equiv \chi_{e,t=t_{0+}} - \chi_{e,t=t_{0-}}$, across the transition at $t = t_0$ was given enough accurately by a simple equation [5]

$$\delta\chi_e(r) = \frac{3}{2}\frac{1}{n_e \nabla T_e A}\int_0^V n_e\,\delta\left(\frac{\partial T_e}{\partial t}\right) dV, \qquad (5)$$

where A and V are the surface area and the enclosed volume at the radius r, respectively. The jump of $\partial T_e/\partial t$, $\delta(\partial T_e/\partial t) \equiv (\partial T_e/\partial t)_{t=t_{0+}} - (\partial T_e/\partial t)_{t=t_{0-}}$, is clearly found in Fig. 10 for 6th and 7th channels, whose values are roughly obtained as -(25±3) keV/s for 6th channel and -(17±3) keV/s for 7th channel. The value of ∇T_e between $r = r_{e6} = 0.5$ m and $r = r_{e7} = 0.4$ m is about -10 keV/m. Because of the limited data for $n_e(r)$ and $\partial T_e(r)/\partial t$, the jump $\delta\chi_e$ can be evaluated only approximately. Assuming that the product of n_e and $\delta(\partial T_e/\partial t)$ is proportional to $(r/r_1)^\alpha$ in the region of $r < r_1$, Eq. (5) is rewritten as

$$\delta\chi_e(r) \cong \frac{3\,r}{2\,(2+\alpha)\,\nabla T_e}\,\frac{n_e(r_1)}{n_e(r)}\,\left(\frac{r}{r_1}\right)^\alpha\,\delta\left(\frac{\partial T_e}{\partial t}\right)_{r=r_1}\,. \qquad (6)$$

Inserting obtained values of $\delta(\partial T_e/\partial t)$ and ∇T_e to this equation, we calculate the $\delta\chi_e$ value at the position of 6th channel r = 0.5 m as about $1.0 / (1+0.5\alpha)$ m^2/s. The power α is considered between 0 and 1, and the jump of χ_e near the ITB is estimated as $\delta\chi_e = (0.6 \sim 1.0)$ m^2/s.

This degraded transport is soon varied to the improved one. The discontinuous change in the time derivative dT_e/dt are clearly seen twice on T_{e6} and T_{e7} simultaneously at the times C (t = 5.968 s) and D (t = 6.015 s). At the second recovery transition, the discontinuous increase of T_{e13} is clearly seen simultaneously with that of T_{e6} and T_{e7}. The evolution of W_{dia} is found to be discontinuous also at these times. The increase of W_{dia} starts again from the second transition, when a small $D\alpha$ decay is noticed. On the other hand, in the region out of ITB, r/a > 0.6, decrease of T_e is observed after these recovery transitions. This is because the energy flow through this region is decreased by the formation of the ITB. As for the T_i response during this recovery phase, the breakdown of diagnostic beam around t = 6.05 s and the slow time resolution make us difficult to know them.

The absolute values of $\delta(\partial T_e/\partial t)$ during this recovery phase is smaller than that at the time B (t = 5.921 s) for the H-L back transition, and values of $|\delta\chi_e|$ near r = 0.5 m at the times C (t = 5.968 s) and D (t = 6.015 s) are estimated as 1/2 ~ 1/3 of that at the time B. After these two times of recovery, the value of χ_e near the ITB region becomes again as small as that before the H-L back transition. We suppose that the ITB properties are reformed.

We find from above analysis that the reduction of $\delta\chi_e$ during the recovery transition (or the reformation of ITB) occurs in the fast time scale shorter than 10 ms. Study of the time scale of the first formation of ITB will be done in future.

5. Discussion

The physics of RS discharges has not fully been understood yet. In JT-60U, the ITB structures are clearly seen not only for T_i and n_e but for T_e. The profiles of T_i, T_e and n_e is remarkably flat in the core region inside the ITB [1]. The non-simultaneous destruction of enhanced particle confinement and improved ion confinement was noticed for TFTR RS plasmas [15]. This suggests that there are plural mechanisms involved in the RS enhanced confinement. Little reduction of the χ_e value was seen for TFTR RS discharges in contradiction to JT-60U results. In DIII-D RS plasmas, there was also no significant improvement in χ_e and the heat losses through electron conductivity was dominant [16].

In the present paper, we found that the positions of ITB for T_i and T_e are located at different positions with each other in JT-60U. Different mechanisms could work to form the ion ITB and electron ITB. To prove this difference, the more accurate analyses will be necessary in future with the more accurate equilibrium calculations as was mentioned in subsection 3.3.

Steep features of the ITB in RS plasmas were studied by reconstructing "real" profiles during programmed motion phase, because the number of diagnostic channels is limited to obtain the steep structure at once. Understanding of the ITB properties depends strongly on the accurate measurement of the ITB structures. The uncertainty in the reconstruction of the "real" profile from "measured" one originates mainly from the difficulty of estimating $\partial T/\partial t$ in the RHS of Eqs. (3) and (4).

Now we can propose a new experimental technique to measure the steep structure of the ITB. In order to estimate the value of $\partial T/\partial t$ and to eliminate the uncertainty, it will be necessary to introduce the non-monotonic plasma motion shown by a dashed curve in Fig. 13 instead of the monotonic motion used in previous RS discharges (a solid curve). We call this style of non-monotonic motion a "multi-step programmed motion". Two identical discharges will be operated, but have different programmed motions, monotonic and "multi-step" ones. The comparison of such a pair of pulses or even the analysis of one case with multi-step motion can resolve the $\partial T_e/\partial t$ value rather accurately.

By introducing this technique to future experiments in JT-60U, we will clarify the structures and characteristics of the ITB in RS plasmas as well as normal shear plasmas.

6. Summary

Characteristics of the ITB structure for reversed shear (RS) plasmas as well as for normal shear plasmas in JT-60U are studied.

5. Discussion

The physics of RS discharges has not fully been understood yet. In JT-60U, the ITB structures are clearly seen not only for T_i and n_e but for T_e. The profiles of T_i, T_e and n_e is remarkably flat in the core region inside the ITB [1]. The non-simultaneous destruction of enhanced particle confinement and improved ion confinement was noticed for TFTR RS plasmas [15]. This suggests that there are plural mechanisms involved in the RS enhanced confinement. Little reduction of the χ_e value was seen for TFTR RS discharges in contradiction to JT-60U results. In DIII-D RS plasmas, there was also no significant improvement in χ_e and the heat losses through electron conductivity was dominant [16].

In the present paper, we found that the positions of ITB for T_i and T_e are located at different positions with each other in JT-60U. Different mechanisms could work to form the ion ITB and electron ITB. To prove this difference, the more accurate analyses will be necessary in future with the more accurate equilibrium calculations as was mentioned in subsection 3.3.

Steep features of the ITB in RS plasmas were studied by reconstructing "real" profiles during programmed motion phase, because the number of diagnostic channels is limited to obtain the steep structure at once. Understanding of the ITB properties depends strongly on the accurate measurement of the ITB structures. The uncertainty in the reconstruction of the "real" profile from "measured" one originates mainly from the difficulty of estimating $\partial T/\partial t$ in the RHS of Eqs. (3) and (4).

Now we can propose a new experimental technique to measure the steep structure of the ITB. In order to estimate the value of $\partial T/\partial t$ and to eliminate the uncertainty, it will be necessary to introduce the non-monotonic plasma motion shown by a dashed curve in Fig. 13 instead of the monotonic motion used in previous RS discharges (a solid curve). We call this style of non-monotonic motion a "multi-step programmed motion". Two identical discharges will be operated, but have different programmed motions, monotonic and "multi-step" ones. The comparison of such a pair of pulses or even the analysis of one case with multi-step motion can resolve the $\partial T_e/\partial t$ value rather accurately.

By introducing this technique to future experiments in JT-60U, we will clarify the structures and characteristics of the ITB in RS plasmas as well as normal shear plasmas.

6. Summary

Characteristics of the ITB structure for reversed shear (RS) plasmas as well as for normal shear plasmas in JT-60U are studied.

The fast-time-scale outward expansion of the ITB position is seen at the phase q_{min} passes across 3 in RS discharges. Some not well expressed or better visible acceleration of toroidal rotation is seen also.

The steep features of the T_e and T_i profiles in RS plasmas are measured during the programmed-motion phase. The position of the "shoulder" of ITB is determined with high space resolution. The width of the ITB is smaller than 10 cm. The discontinuous change of χ_e within 3 cm distance near the ITB "shoulder" is found and the χ_e value in the ITB region is 1/10 of that inside the ITB "shoulder". It is observed that locations of the ITB for T_e and T_i are slightly different from each other. This reason should be clarified in future.

The BLM-induced L-H transition and the H-L back transition in a high β_p plasma with normal shear are studied. The BLM suddenly relaxes the T_e profile but does not deteriorate the improved transport property. The H-L back transition causes the simultaneous degradation of transport near the ITB region. The χ_e jump near the ITB is estimated as about 1 m^2/s. After the back transition, the transport is discontinuously improved in time and the ITB properties are recovered. The time scale of this recovery transition is shorter than 10 ms. Global natures of these transient processes are noticeable.

A new experimental technique called "multi-step programmed motion" is proposed to measure the steep structure of the ITB. The "real" structure will be reconstructed more accurately from the "measured" profile by using this method.

Acknowledgments

The authors are grateful for the collaboration with members of the JT-60 team. They especially acknowledge Dr. A. Polevoi for fruitful discussion. This work was carried out when one of the authors (S.V.N.) was visiting JAERI as an ISTC Research Fellow during January 12 to April 11, 1997. He is indebted to staffs of JAERI for their kind hospitality.

The fast-time-scale outward expansion of the ITB position is seen at the phase q_{min} passes across 3 in RS discharges. Some not well expressed or better visible acceleration of toroidal rotation is seen also.

The steep features of the T_e and T_i profiles in RS plasmas are measured during the programmed-motion phase. The position of the "shoulder" of ITB is determined with high space resolution. The width of the ITB is smaller than 10 cm. The discontinuous change of χ_e within 3 cm distance near the ITB "shoulder" is found and the χ_e value in the ITB region is 1/10 of that inside the ITB "shoulder". It is observed that locations of the ITB for T_e and T_i are slightly different from each other. This reason should be clarified in future.

The BLM-induced L-H transition and the H-L back transition in a high β_p plasma with normal shear are studied. The BLM suddenly relaxes the T_e profile but does not deteriorate the improved transport property. The H-L back transition causes the simultaneous degradation of transport near the ITB region. The χ_e jump near the ITB is estimated as about 1 m^2/s. After the back transition, the transport is discontinuously improved in time and the ITB properties are recovered. The time scale of this recovery transition is shorter than 10 ms. Global natures of these transient processes are noticeable.

A new experimental technique called "multi-step programmed motion" is proposed to measure the steep structure of the ITB. The "real" structure will be reconstructed more accurately from the "measured" profile by using this method.

Acknowledgments

The authors are grateful for the collaboration with members of the JT-60 team. They especially acknowledge Dr. A. Polevoi for fruitful discussion. This work was carried out when one of the authors (S.V.N.) was visiting JAERI as an ISTC Research Fellow during January 12 to April 11, 1997. He is indebted to staffs of JAERI for their kind hospitality.

References

[1] T. Fujita, S. Ide, H. Kimura, Y. Koide, T. Oikawa, S. Takeji, H. Shirai, T. Ozeki, Y. Kamada, S. Ishida, the JT-60 Team, 16th IAEA Fusion Energy Conference, Montreal, 1996, IAEA-CN-64/A1-4.

[2] Y. Koide, JT-60 Team, Phys. Plasmas **4** (1997) 1623.

[3] T. Fukuda, M. Sato, T. Takizuka, K. Tsuchiya, Y. Kamada, H. Takenaga, the JT-60 Team, 16th IAEA Fusion Energy Conference, Montreal, 1996, IAEA-CN-64/AP2-9.

[4] Y. Koide, S. Ishida, M. Kikuchi, M. Mori, S. Tsuji et al., in Plasma Physics and Controlled Nuclear Fusion Research 1994 (Proc.14th Int. Conf., Sevillie, 1994), Vol. 1, IAEA, Vienna (1995) 199.

[5] S.V. Neudatchin, T. Takizuka, H. Shirai, N. Isei, Y. Kamada, Y. Koide, M. Sato, M. Azumi, Jpn. J. Appl. Phys. **35** (1996) 3595.

[6] H. Shirai, T. Takizuka, M. Sato, Y. Koide, T. Hirayama, in Controlled Fusion and Plasma Physics (Proc. 23rd EPS Conf. Kiev, 1996), Vol. 20C, Part 1, EPS, Geneva (1996) 339.

[7] H. Shirai, T. Takizuka, Y. Koide, Y. Kamada, S. Ishida, M. Mori, O. Naito, M. Sato, N. Isei, T. Fukuda, Y. Kawano, T. Hirayama, M. Azumi, Plasma Phys. Contr. Fusion **38** (1996) 1455.

[8] S. Ishida, A. Nagashima, M. Sato, N. Isei , T. Matoba, Rev. Sci. Instrum. **61** (1990) 2864.

[9] Y. Koide, S. Ishida, A. Sakasai, H. Shirai, T. Hirayama, H. Kubo, T. Sugie, A. Funahashi , Nucl. Fusion **33** (1993) 251.

[10] T. Fujita et al., "High Performance Reversed Shear Plasmas with Large Radius Transport Barrier in JT-60U", in preparation to be submitted to Nucl. Fusion.

[11] S. Takeji, Y. Kamada, T. Ozeki, S. Ishida, T. Takizuka, Y. Neyatani, S. Tokuda, JT-60 Team, in Controlled Fusion and Plasma Physics (Proc. 22nd EPS Conf. Bournemouth, 1995), Vol. 19C, Part IV, EPS, Geneva (1995) 33;
S. Takeji, Y. Kamada, T. Ozeki et al., "MHD Analysis of Instabilities Associated with ITB", in "Review of JT-60U Experimental Results from February to October, 1995", JAERI-Research 96-018 (1996) pp. 52 - 55.

[12] S. Takeji, Y. Kamada, T. Ozeki, S. Ishida, T. Takizuka, Y. Neyatani, S. Tokuda, " Ideal Magnetohydrodynamic Instabilities with Low Toroidal Mode Numbers Localized near an Internal Transport Barrier in JT-60U High-β_p Mode Plasmas", submitted to Phys. Plasmas.

[13] H. Shirai, T. Hirayama, K. Shimizu, K. Tani, M. Azumi, K. Takase, Y. Tahata, K. Hirai, "Outline and Handling Manual of Experimental Data Time Slice Monitering Software SLICE", JAER-M 93-026 (1996) (in Japanese); H. Shirai et al., in preparation to submitt to JAERI-CODE.

[14] Y. Koide, T. Takizuka S. Takeji, S. Ishida, M. Kikuchi, Y. Kamada, T. Ozeki, Y. Neyatani, H. Shirai, M. Mori, S. Tsuji-Iio, Plasma Phys. Control. Fusion **38** (1996) 1011.

[15] F.M. Levinton, S.H. Batha, M. Beer, M.G. Bell, R.E. Bell et al., 16th IAEA Fusion Energy Conference, Montreal, 1996, IAEA-CN-64/A1-3.

[16] D.P. Schissel, C.M. Greenfield, J.C. DeBoo, L.L. Lao, E.A. Lazarus et al., 16th IAEA Fusion Energy Conference, Montreal, 1996, IAEA-CN-64/A5-3.

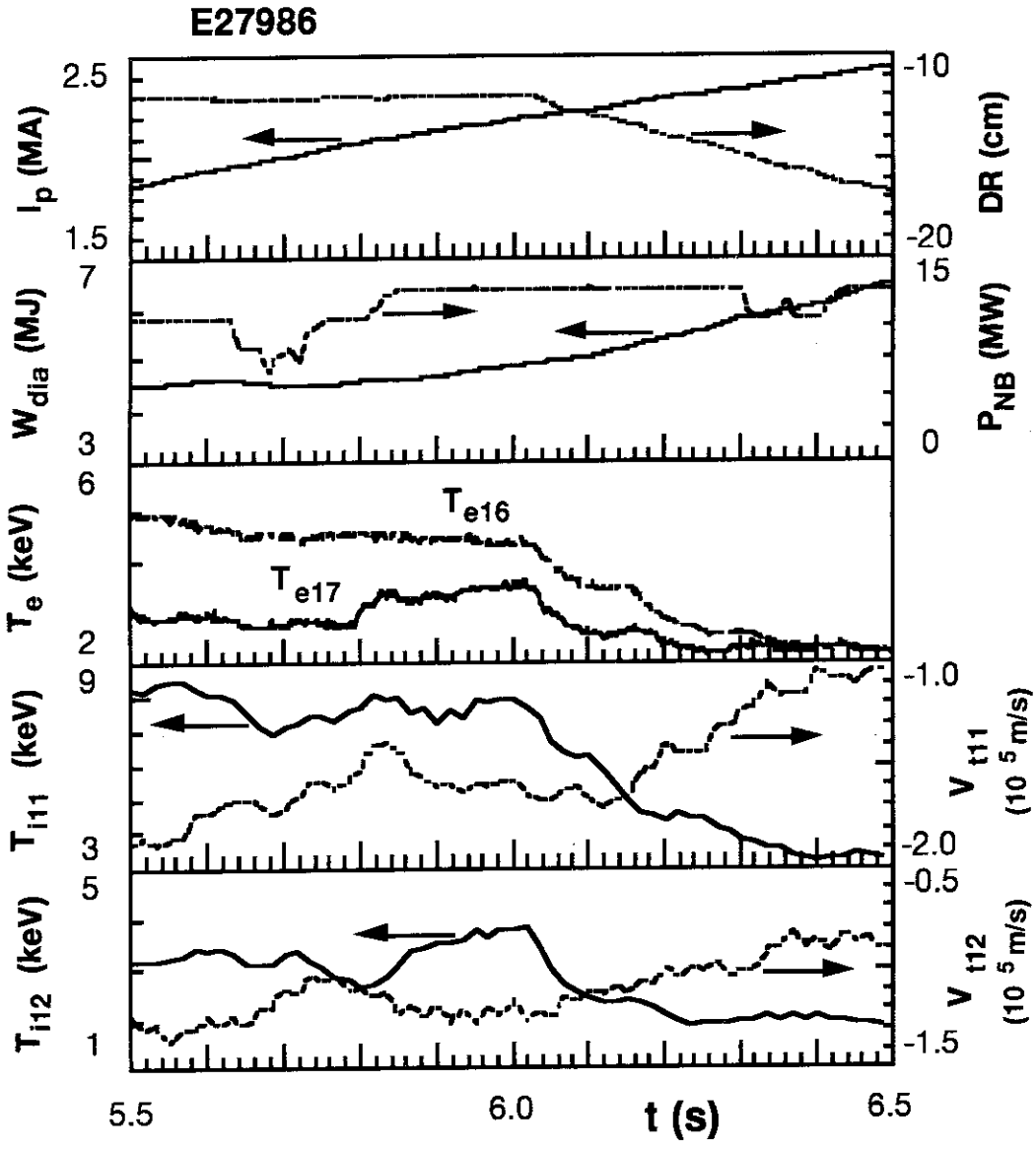

Fig. 1 Waveforms of the RS discharge E27986. Plasma current I_p, displacement of plasma center in the major-radius direction DR, stored energy measured by diamagnetic loop W_{dia}, injected neutral beam power P_{NB}, electron temperature T_e, ion temperature T_i, and toroidal rotation velocity V_t are shown. An ITB expansion before t = 6.0 s is described in section 2 and the programmed motion after t = 6.0 s is described in section 3.

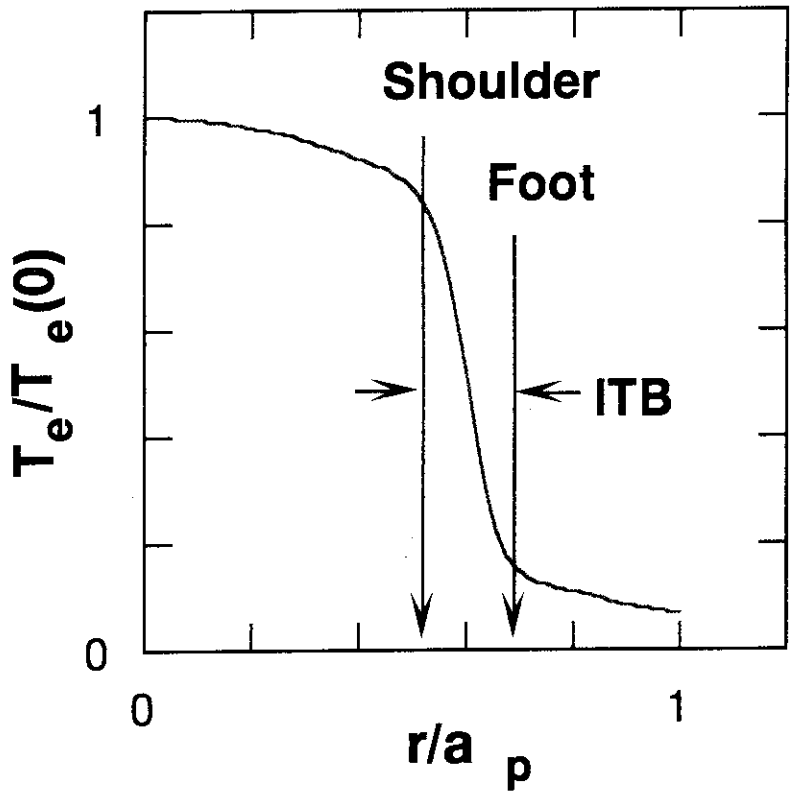

Fig. 2 Schematic profile of ITB. Outer boundary of the ITB is called the "foot", and the inner boundary is called the "shoulder".

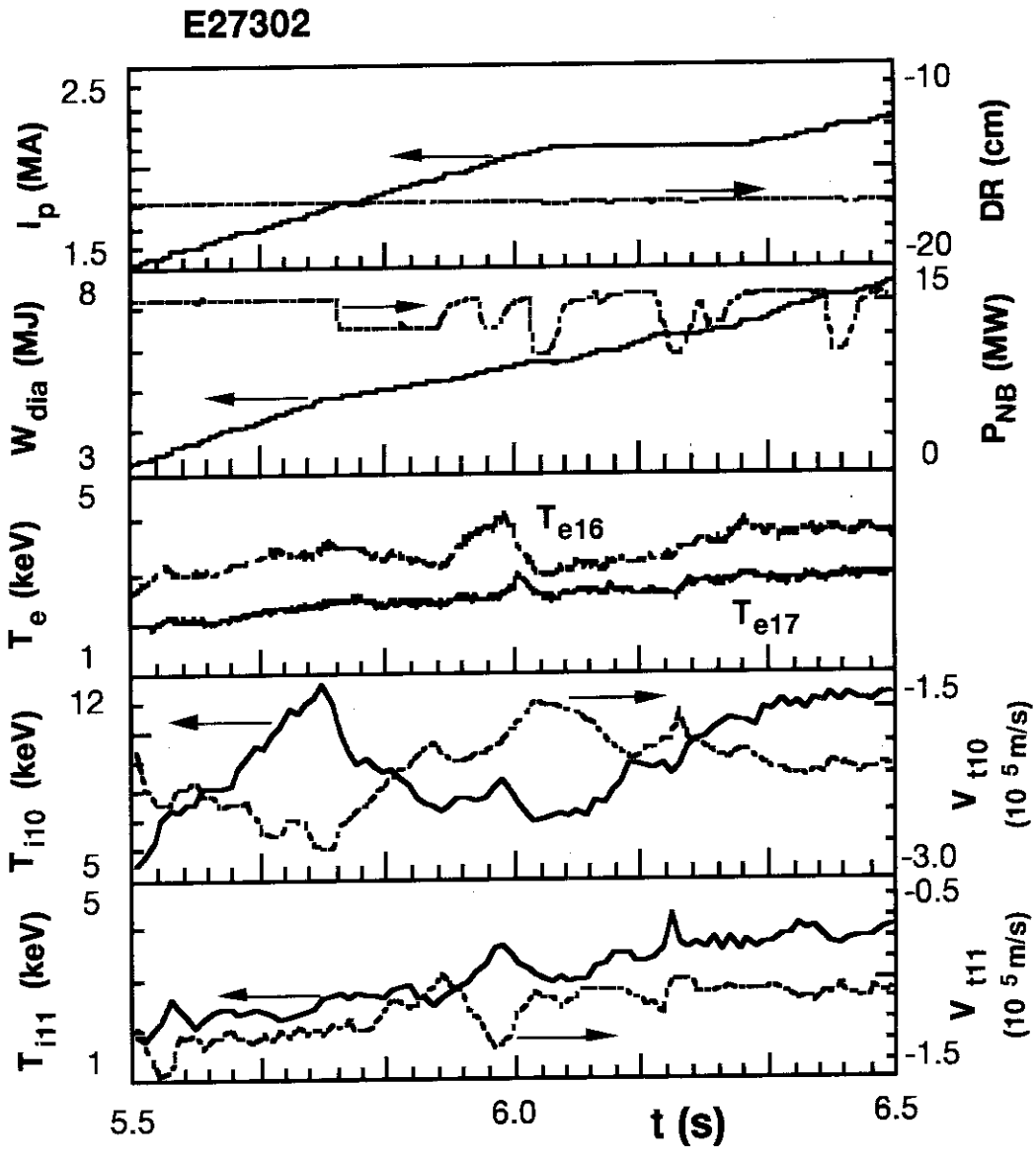

Fig. 3 Waveforms of the RS discharge E27302. A relaxation of ITB gradient at t = 5.4 s and an expansion of ITB position at t = 5.6 s are seen.

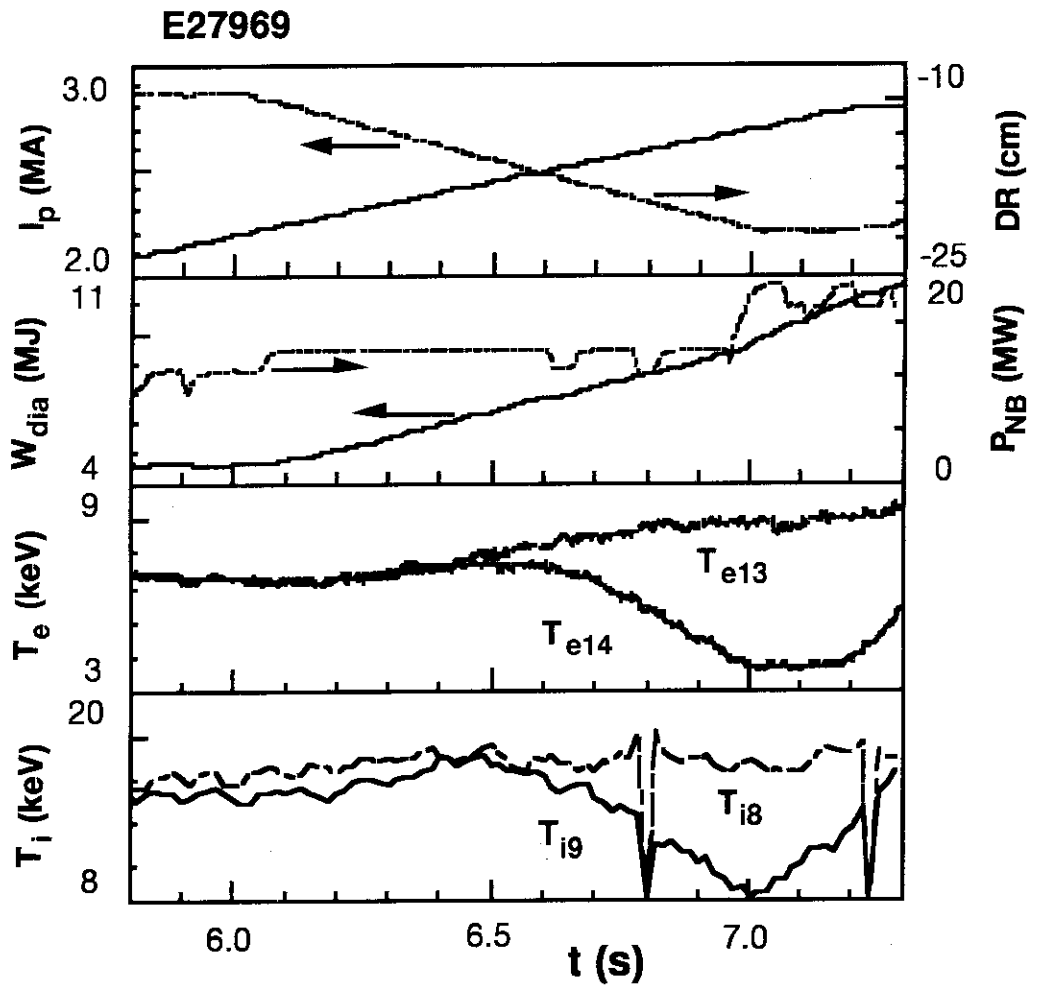

Fig. 4 Waveforms of the RS pulse E27969 (the highest Q_{DT}^{eq} shot). Different evolutions between T_{e13} and T_{e14} , and between T_{i8} and T_{i9} are clearly seen during the programmed motion phase.

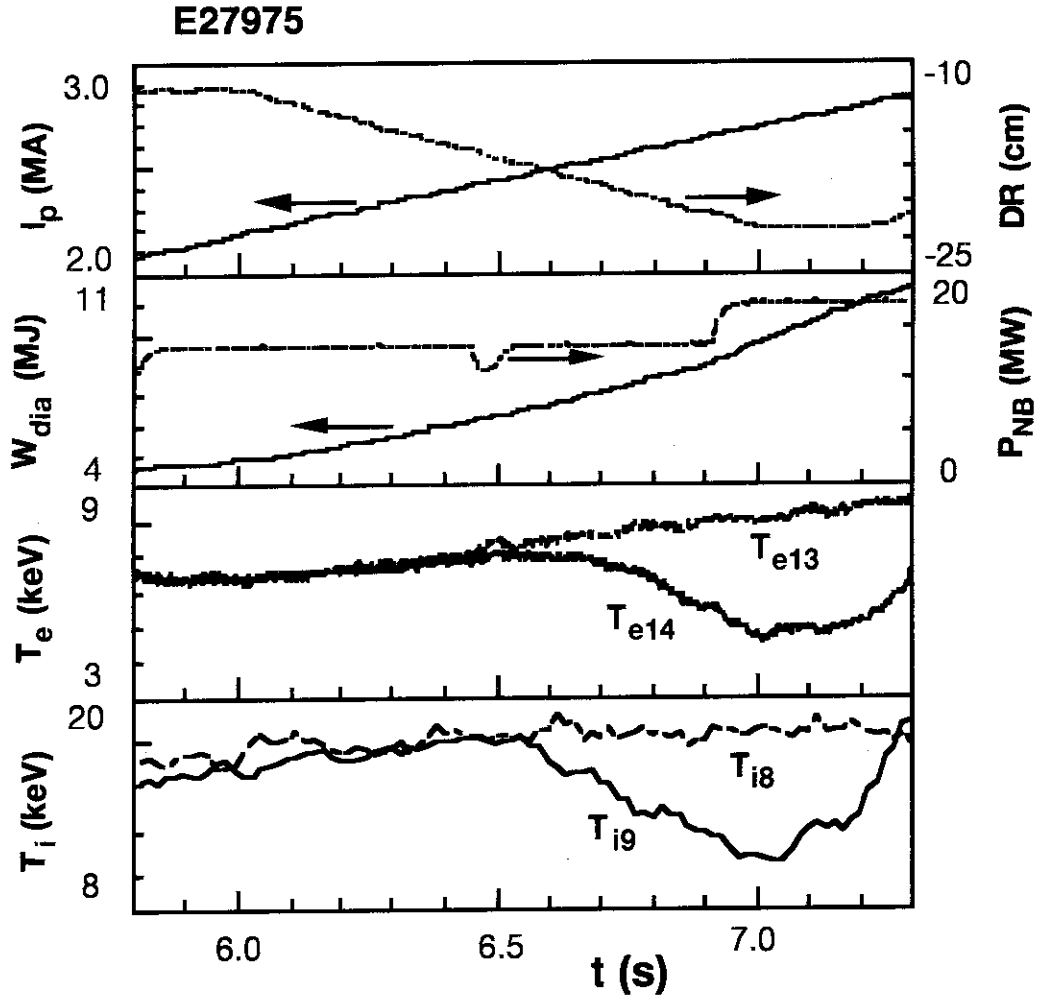

Fig. 5 Waveforms of the RS pulse E27975. Behaviors similar with E27969 are reproducibly obtained.

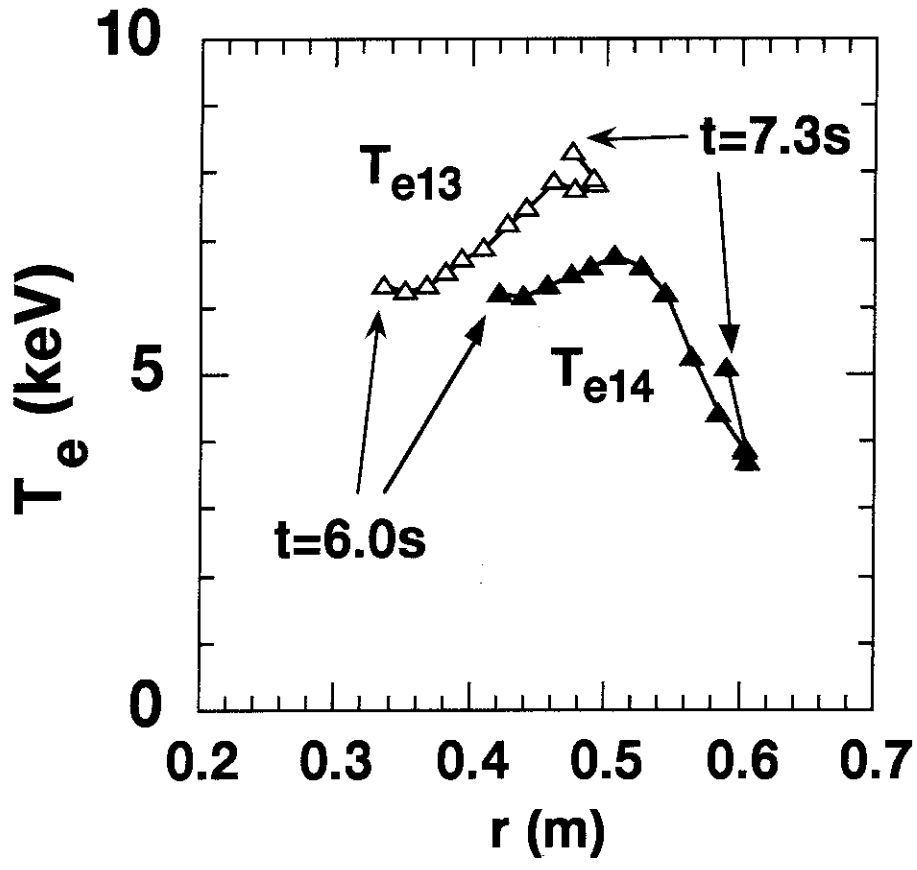

Fig. 6 Evolution of radial positions and T_e values for 13th and 14th channels in a moving plasma of E27969. The ITB feature is seen on the track of T_{e14}. Points on a curve from inner to outer are plotted at every 0.1 s from t = 6.0 s to t = 7.3 s.

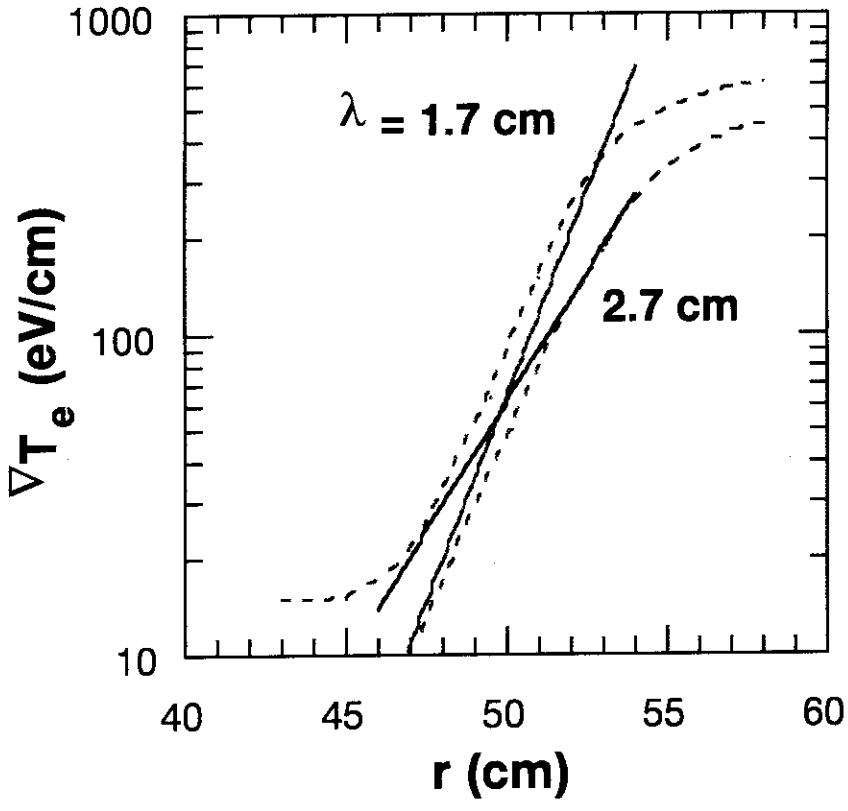

Fig. 7 Radial profile of "real" $|\nabla T_e|$ near the ITB "shoulder" in E27969. A possible band of the profile is given. The characteristic length, $\lambda \equiv \nabla T_e / \nabla (\nabla T_e)$, is (2.2 ± 0.5) cm.

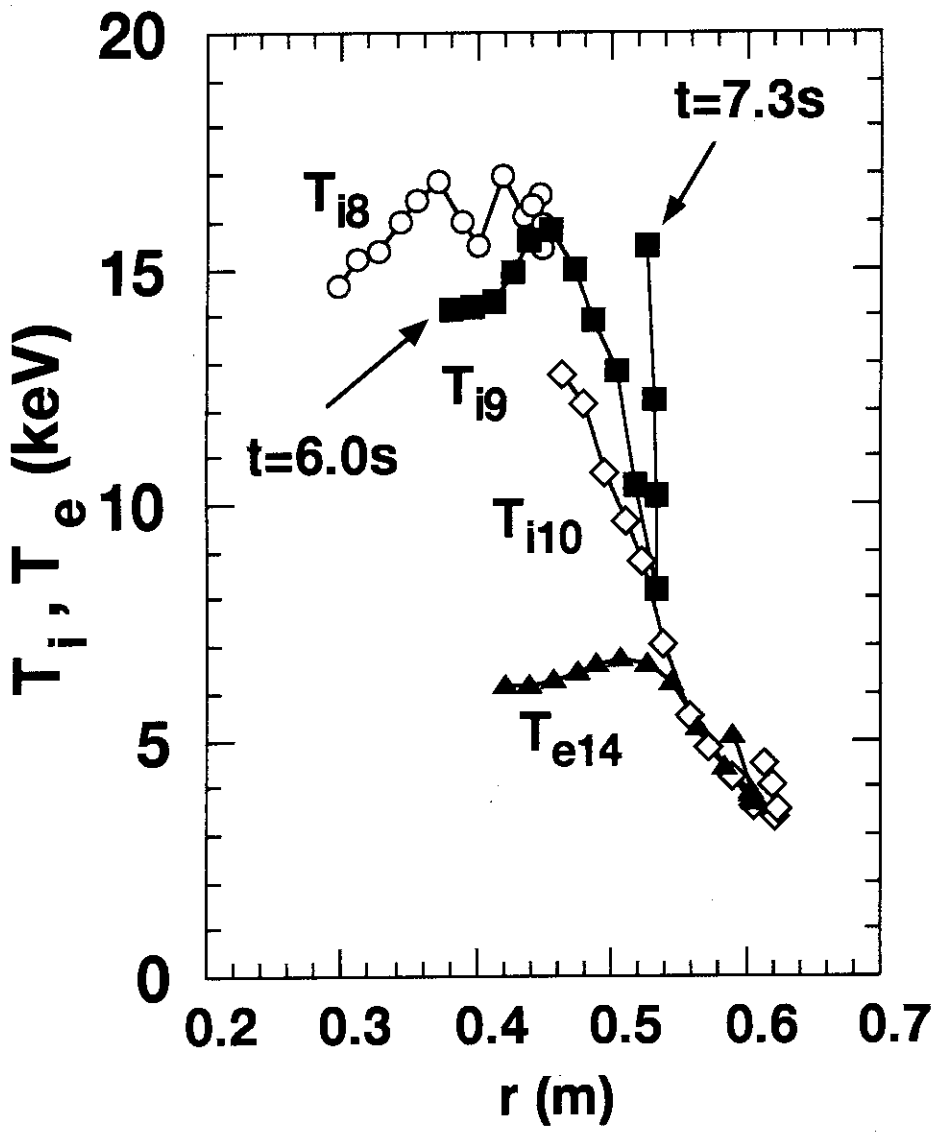

Fig. 8 Evolution of radial positions and T_i values for channels 8, 9 and 10 in the shot E27969. The T_{e14} data from Fig. 6 are also presented for comparison.

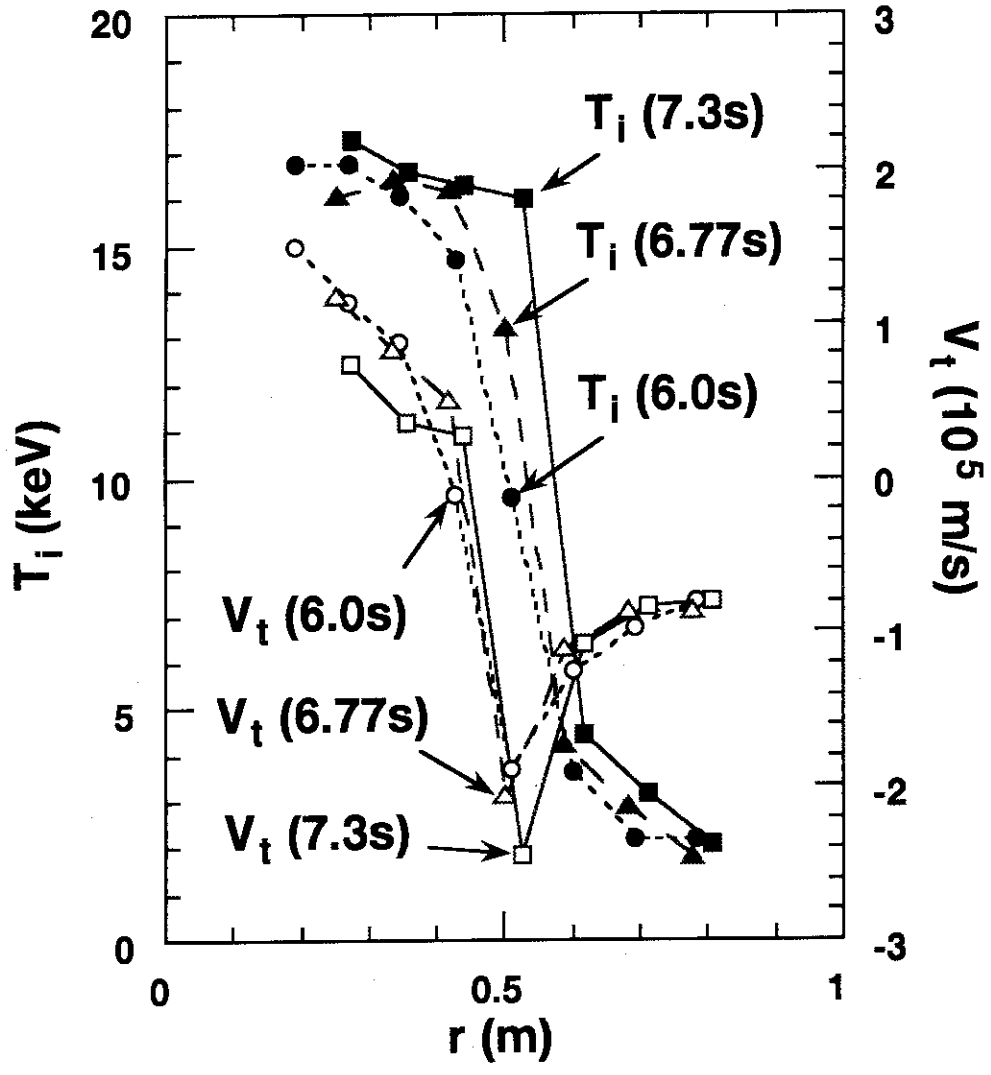

Fig. 9 Radial profiles of T_i (closed symbols) and V_t (open symbols) for E27969. They are obtained from many channels at three moments, t = 6.0 s (dotted curve), 6.77 s (dashed curve) and 7.3 s (solid curve).

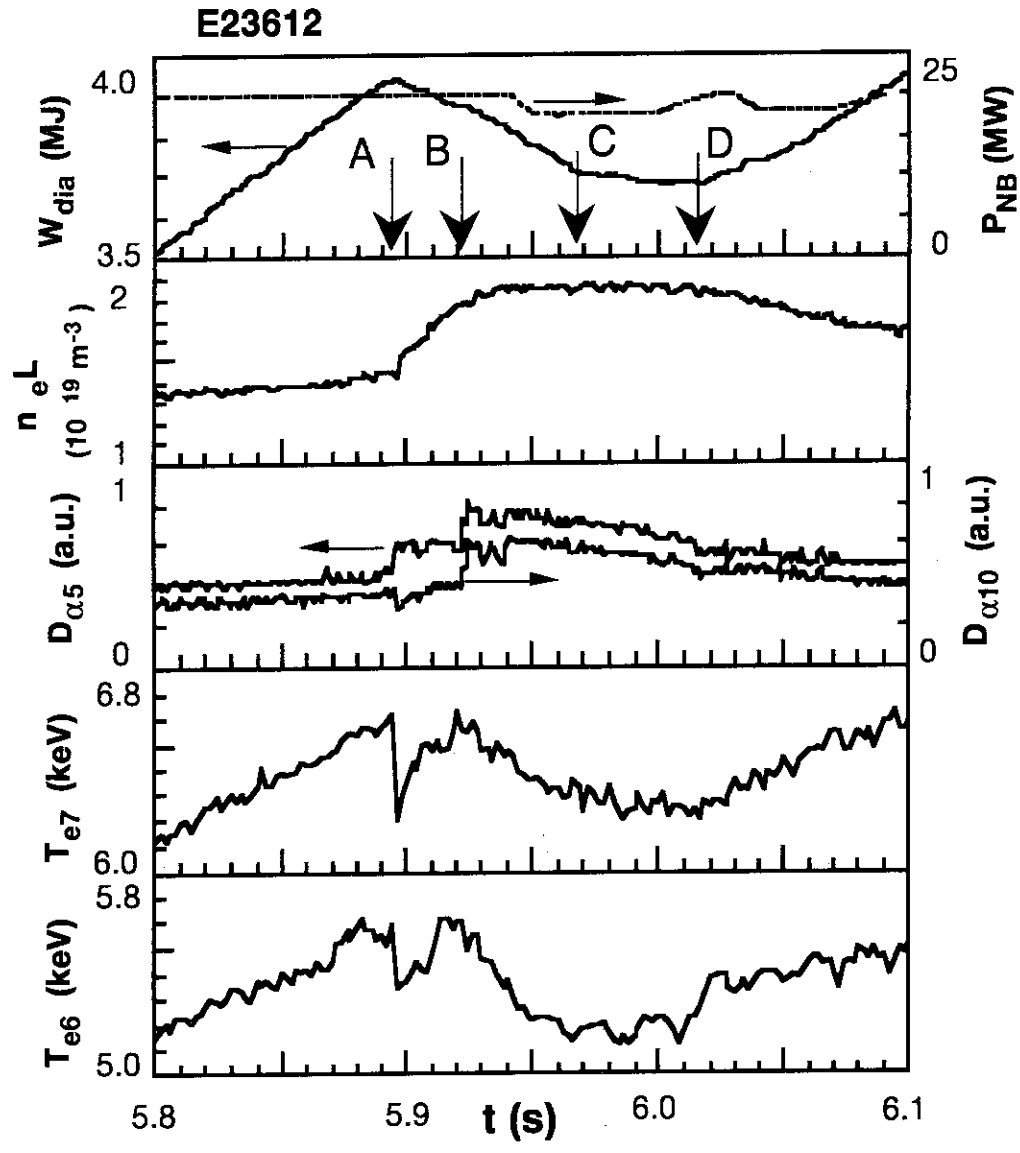

Fig. 10 Waveforms of the high β_p discharge E23612 of normal shear plasma. Stored energy measured by diamagnetic loop W_{dia}, injected neutral beam power P_{NB}, line integrated electron density n_eL, D_α signals from ($D_{\alpha 10}$) and away from ($D_{\alpha 5}$) the divertor region, and electron temperature T_e for channels 7 and 6 are shown. Arrows indicate the times of transitions ; A) BLM at t = 5.895 s, B) H-L back transition at t = 5.921 s, C) first recovery at t = 5.968 s, and D) second recovery at t = 6.015 s.

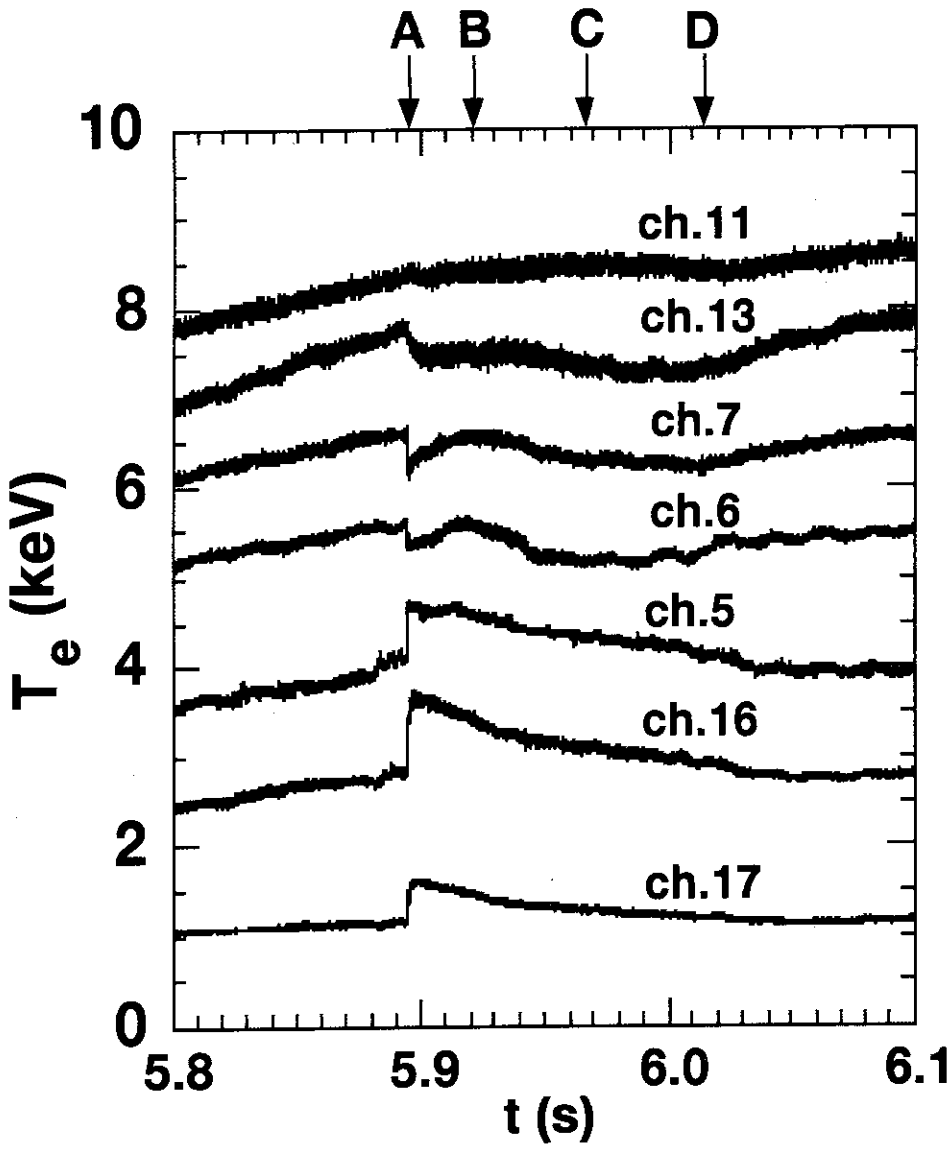

Fig. 11 Time evolution of T_e at $r/a_p = 0.14$ (ch. 11), $r/a_p = 0.33$ (ch. 13), $r/a_p = 0.44$ (ch. 7), $r/a_p = 0.56$ (ch. 6), $r/a_p = 0.68$ (ch. 5), $r/a_p = 0.79$ (ch. 16), and $r/a_p = 0.98$ (ch. 17). Arrows mean the same as those in Fig. 10.

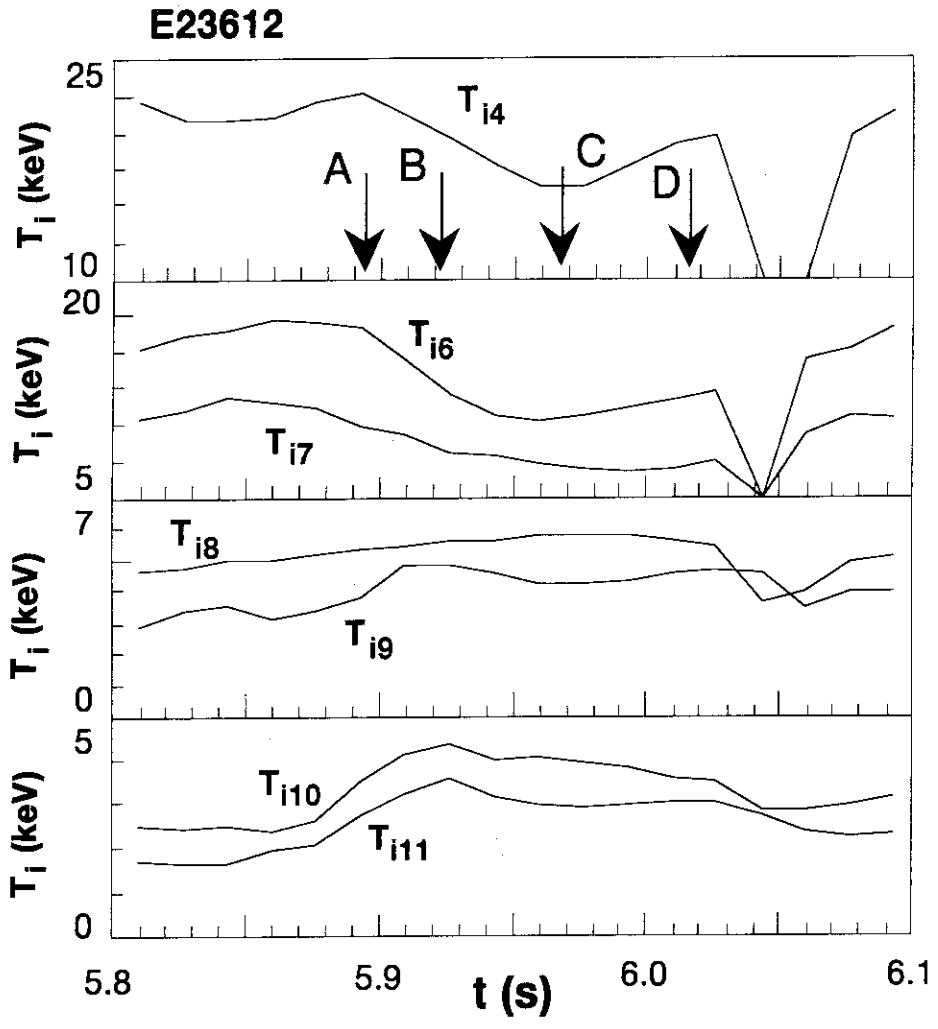

Fig. 12 Time evolution of T_i at r/a_p = 0.31 (ch. 4), r/a_p = 0.43 (ch. 6), r/a_p = 0.53 (ch. 7), r/a_p = 0.63 (ch. 8), r/a_p = 0.74 (ch. 9), r/a_p = 0.85 (ch. 10), and r/a_p = 0.98 (ch. 11). Breakdown of diagnostic beam occurs around t = 6.05 s.

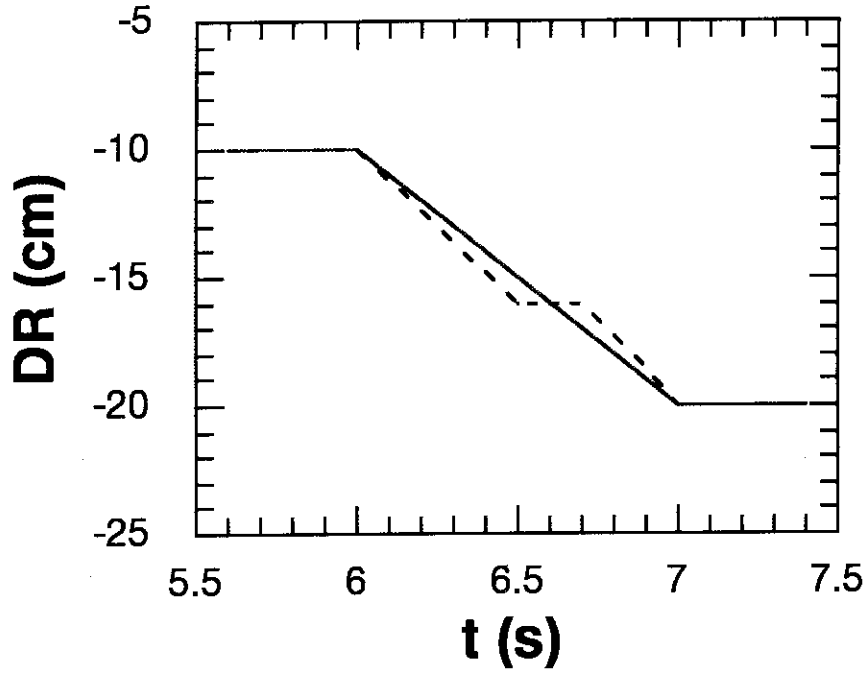

Fig. 13 Displacement of plasma center in the major-radius direction DR. Usually its motion is monotonic in time as shown by a solid curve. To measure the steep structure of the ITB, non-monotonic plasma motion shown by a dashed curve is proposed.